

# Design and Analysis of Grouping Active Subcarrier Frequency-Time Index Modulation for Differential Chaos Shift Keying Communication System

Ruaa Abdulkareem Yaseen, and Fadhil S. Hasan

Original scientific article

**Abstract**—In this paper, an innovative system called grouping frequency-time index modulation-based differential chaos shift keying (GFTIM-DCSK-I) is presented to improve the energy efficiency (EE), spectral efficiency, and data rate of the recently proposed grouping subcarrier index modulation in differential chaos shift keying (GSIM-DCSK) system. The proposed system optimally utilizes both frequency and time resources, enabling efficient transmission at high data rates. The data information bits are divided into equal  $L$  groups, each containing  $(p_1+p_2+1)$  bits. Within each group, the first set of bits, referred to as  $p_1$  bits, are assigned as carrier-indexed bits, whereas the second set of bits, known as  $p_2$  bits, are designated as time-indexed bits. Additionally, one bit is assigned for modulation. The  $p_1$  bits serve as an index selector for choosing a single active subcarrier from a total of  $2^{p_1}$  subcarriers.  $p_2$  bits are utilized to choose a single time slot out of a total of  $2^{p_2}$  available options. The modulated bit undergoes DCSK modulation and is thereafter sent via the active subcarriers. Mathematical expressions are constructed to examine the system performance of energy efficiency, spectral efficiency, and system complexity, then compared with the traditional DCSK modulations. Analytical formulas for the bit error rate (BER) of the proposed system are obtained under the impact of multipath Rayleigh fading channel and additive white Gaussian noise (AWGN). Results from simulations and analysis confirm that the theoretical analysis is accurate. The performance of the suggested approach is also evaluated by comparing it to conventional DCSK techniques, showing an improvement in the performance.

**Index Terms**—frequency index, time index, differential chaos shift keying (DCSK), energy and spectral efficiency, AWGN, multipath Rayleigh fading channel.

## I. INTRODUCTION

THE use of chaotic signals in spread-spectrum communication systems has gained significant popularity

Manuscript received January 12, 2024; revised February 22, 2024. Date of publication May 9, 2024. Date of current version May 9, 2024. The associate editor prof. Giovanni Giambene has been coordinating the review of this manuscript and approved it for publication.

Authors are with the Department of Electrical Engineering, Al-Mustansiriyah University, Baghdad, Iraq (e-mails: {ruaa.k.yaseen, fadel\_sahib}@uomustansiriya.edu.iq).

Digital Object Identifier (DOI): 10.24138/jcomss-2023-0182

due to its simplicity of generating process and exceptional auto-correlation characteristics [1], [2]. Extensive research has been done regarding chaotic communications in wireless communication applications over the past two decades. This is primarily attributed to its advantageous characteristics, such as low power consumption, low complexity implementation, and excellent resistance to fading effects [3]. The chaotic signal exhibits a property known as "sensitive dependence upon initial conditions," which enables the formation of a theoretically unlimited number of uncorrelated signals.

The classification of chaotic modulation schemes is based upon the necessity of chaos synchronization, yielding two different categories: coherent modulation schemes and non-coherent modulation schemes. One potential communication strategy that exhibits chaotic behavior is utilizing chaos as a carrier waveform or spread-spectrum waveform for addressing challenges such as chaotic masking [4].

Chaos shift keying (CSK) [5], [6], are two communication techniques that utilize chaos theory principles. In the context of these applications, it is essential to note that the chaotic waveform does not inherently include information. Rather, the information is concealed inside the chaotic signal using a process known as chaotic masking. Alternatively, in the case of CSK, information is encoded by means of a key shift. In order to retrieve the information, it is typically necessary to employ complicated, chaotic synchronization at the receiver. In order to mitigate the challenges associated with achieving precise synchronization, a proposed system that utilizes a non-coherent receiver has been introduced. This system, known as a differential chaos shift keying (DCSK) system, does not depend on chaotic synchronization on the receiver side to generate an exact replica of the chaotic sequence. Instead, it only necessitates frame or symbol rate sampling [7]. However, it has been observed that the DCSK system exhibits more resilience in the presence of multi-path fading conditions compared to the differential phase shift keying (DPSK) scheme. As a result, it is seen to be well-suited for applications using ultra-wideband (UWB) technology [8]-[11].

The conventional DCSK technique is associated with two

primary drawbacks. Initially, it should be noted that half a portion of the symbol time and energy is allocated for transmitting a reference-chaotic signal, so this leads to the energy efficiency (EE) and data rate being comparatively reduced. Furthermore, the use of radio-frequency (RF) delay lines in the transceiver is a significant challenge due to the inherent limitations of the current complementary metal oxide semiconductor (CMOS) technology. Various modifications to the DCSK system have been proposed to enhance information rate efficiency and save energy. In [12], the authors suggest a method called quadrature chaos shift keying (QCSK) that utilizes the Hilbert transform to generate two sets of orthogonal chaotic functions. This technique allows transmitting a sufficient number of bits compared to DCSK while maintaining the same bandwidth required. In addition, [13] introduces a high-efficiency differential chaos shift keying (HE-DCSK) technique that enhances the data rate by recycling each reference sample of DCSK. In order to transmit several bits using the same reference sequence, researchers have developed three coding schemes: code-shifted differential chaos shift keying (CS-DCSK) [14], generalized code-shifted differential chaos shift keying (GCS-DCSK) [15], and high-data-rate code-shifted differential chaos shift keying (HCS-DCSK) [16]. These schemes utilize Walsh codes and chaotic sequences to generate orthogonal chaotic signals.

Proposed M-ary DCSK versions in [17] – [19] incorporated a novel scenario and parameters of constellations to improve DCSK performance. In [20], a short reference Direct-Sequence with differential chaos shift keying (SR-DCSK) scheme was proposed to enhance data transmission rates and EE. The Gram-Schmidt method is employed in [21] and [22] as an alternative to Walsh code for transmitting several bits at the same time interval.

In [23], a noise reduction DCSK (NR-DCSK) system is used to reduce the influence of noise in the receiving signal by employing a short reference sequence that is repeated  $P$  times and utilized as a reference chaotic sequence.

Multicarrier modulation and orthogonal frequency division multiplexing (OFDM) are used with types of DCSK systems to enhance the EE, spectral efficiency, and information rate of the DCSK system. This results in the following hybrids: OFDM-based short reference quadrature chaos shift keying (OFDM-SRQCSK) [25], multicarrier-based DCSK (MC-DCSK) [8], OFDM-based DCSK (OFDM-DCSK) [24], and OFDM-based OCVSK (OFDM-OCVSK) [26].

In recent years, as a viable contender within the realm of digital modulation techniques for forthcoming wireless communication systems, the idea of index modulation (IM) has been presented [27]. IM uses the indices of specific transmission entities to transmit extra information bits. The aim of these IM-based techniques is to improve the EE and data rate of future wireless communication devices. In recent years, scholarly investigations have extensively examined utilizing specific factors, including space, polarity, code, and frequency, as modulation indices. These indices have been explored to facilitate the transmission of additional bits per symbol while avoiding the need for increased bandwidth or

higher power requirements.

In this work, we propose a grouping frequency-time index modulation-based DCSK (GFTIM-DCSK-I) communication system. The GFTIM-DCSK-I system, as suggested, utilizes both frequency and time resources as index entities. Whereas the recently suggested GSIM-DCSK system [42] just uses the frequency resource as the index entity. So, within the GFTIM-DCSK-I system, it is possible to transmit more additional information bits and save more energy than the GSIM-DCSK system by using the available carrier and time index resources. The GFTIM-DCSK-I system utilizes orthogonal sinusoidal carriers for the transmission of both reference-chaotic and information-bearing signals. In brief, this study outlines the fundamental contributions of the research as follows:

- A novel DCSK communication system called GFTIM-DCSK-I, which is based on grouping frequency-time index modulation, is suggested. This system utilizes two extra dimensions of resources to enhance information transmission. The information bits are partitioned into  $L$  equal groups, each of which contains three parts: the carrier index bits  $p_1$ , the time index bits  $p_2$ , and the modulated bit. In the GFTIM-DCSK-I system, the time slots utilized by the chosen subcarriers send the same index bits. In each sub-group,  $p_1$  bits are used to map symbols to select one active subcarrier from  $2^{p_1}$  subcarriers. Similarly,  $p_2$  bits are employed to map symbols for selecting one out of  $2^{p_2}$  time slots. At the same time, the modulated bit is subjected to modulation via the DCSK technique and, after that, transmitted via the active subcarriers. As a result, during each symbol duration, the amount of bits carried is increased to  $L(p_1+p_2+1)$  bits.
- The system's energy efficiency(EE), spectral efficiency, and complexity analysis are also determined. Comparisons are made between the obtained results and the present traditional DCSK systems, such as MC-DCSK, CI-DCSK, 2CI-DCSK, and GSIM-DCSK-I systems.
- The GFTIM-DCSK-I system's theoretical BER expressions over AWGN and multipath Rayleigh fading channels are also obtained. Both theoretical and simulated results demonstrate that the proposed GFTIM-DCSK-I scheme exhibits a significant enhancement in the bit error rate (BER) performance compared to existing systems such as MC-DCSK, CI-DCSK1, and GSIM-DCSK-I.

The sections that follow in this work are arranged as follows: Section II presents a review of the relevant research. The system model of the proposed GFTIM-DCSK-I scheme is shown in section III. The system analysis is covered in section IV, mainly concentrating on energy efficiency, spectral efficiency, and complexity analysis. The analytic BER of GFTIM-DCSK-I is provided in section V. The numerical results and discussions are provided in section VI. In the end, section VII presents the conclusions.

In the following related work, we show hybrid index modulation approaches with the DCSK families.

## II. RELATED WORKS

In a previous study [28], researchers developed a frequency index modulation (FIM) technique that utilizes frequency rather than the transmit antenna to achieve index modulation. This approach allows for a hardware-friendly implementation.

The proposal in [29] and [30] introduces various families of code index modulation DCSK (CIM-DCSK) schemes. These include code index modulation SR-DCSK (CIM-DCSK), optimized CIM-DCSK, and noise reduction of CIM-DCSK (NR CIM-DCSK). The information bits in CIM-DCSK are split between modulated bits and mapped bits, which are used to indicate an index for the Walsh code. The first time slot is used to deliver a short reference sequence. Following that, the  $P$  replica reference sequence, denoting the sequence-bearing data, is modulated by data bits and a Walsh code that is concurrently selected by the mapped bits. The improvement of CIM-DCSK is achieved by the utilization of optimized CIM-DCSK, where the data-bearing power is adjusted to an optimal value of  $1/P$ . Additionally, NR CIM-DCSK is enhanced when the chaotic sequence is repeated  $P$  times and treated as the reference sequence. These systems have some restrictions since they increase signal energy and transmission length when the mapped bit size increases.

In [31] and [32], a combination of general and multilevel CS-DCSK with CIM is implemented in new DCSK systems (CIM-CS-DCSK and CIM-MCS-DCSK) are proposed. The  $k$ -combinations mapping approach is employed in these systems for the purpose of selecting the indices of Walsh codes.

In [33]–[35], three carrier index DCSK families are proposed: A CI-DCSK with two layers (2CI-DCSK), carrier index M-ary DCSK (CIM-DCSK), and carrier index DCSK (CI-DCSK). In CI-DCSK, the proposal consists of two distinct versions, namely CI-DCSK1 and CI-DCSK2. One subcarrier in CI-DCSK1 is used for the reference sequence, and one active subcarrier is chosen by the mapped bits and carries one bit that's modulated by the DCSK system, while the others are inactive. This system has constraints in which all subcarriers, except two, are inactive. Therefore, this will result in a reduction in the overall system's bandwidth efficiency. In order to improve the efficiency of CI-DCSK1, a new approach called CI-DCSK2 is introduced. This method involves the selection of a single subcarrier by the use of mapped bits, designating it as an inactive subcarrier. The other subcarriers are then allocated for transmitting reference and data-bearing sequences, employing DCSK modulation. The CI-MDCSK system employs the M-ary DCSK modulation technique as a substitute for DCSK modulation, repeating all the scenarios included in the CI-DCSK2 and CI-DCSK1 systems. A 2CI-DCSK system is an adaptation of CI-DCSK1 where the bits of information are separated into two groups, one conveyed via their Hilbert transform and the other via the chaotic sequence. One subcarrier selected by mapped bits is operating in each group. The active subcarrier is responsible for carrying one modulated bit using DCSK modulation. This system exhibits a twofold enhancement in data rate. However, it has the same constraint as CI-DCSK1, wherein only a subset of two or three

subcarriers are actively utilized while the rest of the subcarriers stay idle.

In [36], the authors propose a system referred to as CFIM, which incorporates a combination of code-based and frequency-based index modulation techniques. The sent bits are split into  $K$  blocks, each individual block being designed using a combination of joint code and frequency index by M-ary modulation. One of the drawbacks of this technique is the necessity for synchronization, as the absence of a reference chaotic sequence requires it. Additionally, the receiver must employ channel state information and equalization techniques to mitigate the effects of the multipath fading channel.

A Commutation code index DCSK (CCI-DCSK) and permutation code index DCSK (PI-DCSK) are suggested in [37] and [38], respectively. In CCI-DCSK, Within the same time slot, the reference signal and the information conveying the commutation version chosen by mapped bits are sent. In the PI-DCSK communication scheme, the transmitted signal is partitioned into two distinct time slots. The first time slot is dedicated to carrying the reference sequence, while the second time slot is allocated for transmitting a modulated bit. This modulated bit is transmitted using a duplicate of the original reference sequence that has undergone a permutation process. The mapped bits select each permutation. The disadvantage of these techniques is that the orthogonality of the basis formed by commutation and permutation is not entirely orthogonal, considerable interference arises at large mapped bit sizes, and extended chaotic sequence lengths are required.

In [39], to transmit more information bits, a novel DCSK with multidimensional index modulation (MIM-DCSK) has been suggested. MIM-DCSK takes use of the three dimensions of the transmission entities—the time slot, carrier, and Walsh code. Despite significant research on MIM-assisted DCSK methods, these systems have comparatively high levels of complexity. A communication system called HIM-MC-DCSK is suggested in [40] to enhance the energy efficiency, spectral efficiency, and data rates of IM-DCSK systems by using MC-DCSK with hybrid index modulation (HIM). The HIM-MC-DCSK system utilizes two orthogonal signals to encode the active and inactive subcarriers. Utilizing all subcarriers in the system for transmitting modulated bits boosts the transmission data rate and prevents the inefficient use of spectrum resources.

In [41], a system based on index-modulation-aided DCSK that utilizes both frequency and time resources (CTIM) in order to enhance transmission reliability while reducing complexity is suggested. The CTIM-DCSK system utilizes orthogonal sinusoidal carriers for the transmission of both the reference-chaotic and information-bearing signals. Furthermore, the suggested method allows for the transmission of additional information bits by using the available carrier-and-time index resources. The CTIM-DCSK system shows good performance in terms of data rate and BER. This is attributed to the use of two novel transmission resource domains. At the receiver, a noise reduction operation is employed to further enhance the BER performance of this system.

In [42], two proposed systems for grouping subcarriers using index modulation-based DCSK are denoted as GSIM-DCSKI and GSIM-DCSKII systems. The data bits are partitioned into equal  $L$  groups, each comprised of  $(p_1+p_2)$  bits. Within each group,  $p_1$  bits are designated as indexed bits, while  $p_2$  bits are allocated for modulated bits. Out of  $2^p$  index subcarriers, the indexed bits are utilized as an index selector to choose one active subcarrier (GSIM-DCSK-I) or one inactive subcarrier (GSIM-DCSK-II). On the other hand, DCSK modulation is used to modulate the modulated bits. As a result, the number of sent bits is augmented to  $L(p_1+p_2)$  bits per symbol duration. This system exhibits superior BER performance due to its effective analysis of both energy and data. Moreover, this system has the lowest complexity per bit when compared to conventional DCSK systems such as CI-DCSK, 2CI-DCSK, and MC-DCSK.

Two novel GSIM-DCSK with PI modulation schemes, namely GSPIM-DCSKI and GSPIM-DCSKII, are proposed in [43] For enhancing the energy, spectral efficiency, and data rate. In both methods, one subcarrier carries the reference chaotic sequence. The entire number of input bits is partitioned among the various subcarriers, resulting in the formation of  $G$  groups. The data information bits within each group are divided into three categories: transmitted modulated bits, carrier index bits, and permutation index bits. In GSPIM-DCSKI and GSPIM-DCSKII systems, the carrier index bits' map is the symbol that selects one active or inactive subcarrier from each subgroup's overall subcarrier index, respectively, and the permutation index bits map is the symbol to generate permuted copies of the reference chaotic sequence by choosing one specified permutation operator from among all the permutation operators in the permutation generator block.

Active subcarriers transmit the modulated bits after they have been modulated by PI-DCSK.

### III. GFTIM-DCSK-I PROPOSED SYSTEM MODEL

#### A. Transmitter

Fig. 1 shows the block diagram of the transmitter system employed in GFTIM-DCSK-I. The first step involves generating a reference-chaotic signal of length  $R$ , denoted as  $x_k = [x_1, x_2, \dots, x_R]$ , by employing a second-order Chebyshev polynomial function. The simplicity with which this map may produce chaotic sequences is why it was selected. Furthermore, chaotic sequences are normalized to have mean squared values of unity and mean values of zero, i.e.,  $E[x_k] = 0$  and  $E[x_k^2] = 1$ . This function is specified as  $x_{q,k+1} = 1 - 2x_{q,k}^2$  (where  $k = 1, 2, \dots$ ).

The data information bits are divided into equally  $L$  separate groups. Each of these groups consists of  $(p_1+p_2+1)$  bits. In each group,  $p_1$  bits are allocated as subcarrier-indexed bits, while  $p_2$  bits are assigned as time index bits. The remaining single bit is assigned as the modulated bit. Hence, at every  $v^{th}$  symbol period, the overall number of transmitted bits is equal to  $Lp$  bits, where  $p = p_1+p_2+1$ .

The transmitted bits of the  $g^{th}$  group are represented as  $S_v^g$  in each symbol period,  $v$ . These bits can be written  $S_v^g = \{a_{v,(g-1)p+1}, \dots, a_{v,(g-1)p+p_1}, a_{v,(g-1)p+p_1+1}, \dots, a_{v,(g-1)p+p_1+p_2+1}\}$ , this equation applies to any values of  $g$  ranging from 1 to  $L$ . In the  $g^{th}$  sub-block, the modulated bit  $a_{v,(g-1)p+p_1+p_2+1}$ , which has binary values of 0 or 1, is subjected to a polarity conversion procedure. As a result, the variable  $b_v$  assumes values of 1 or -1.

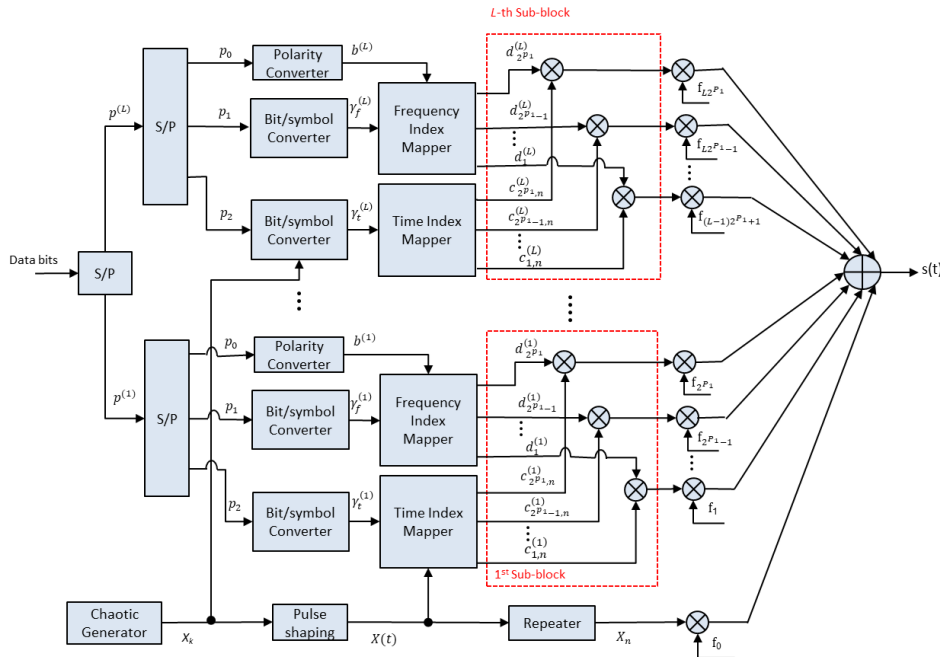


Fig. 1. The structure of the transmitter for the GFTM-DCSK-I system.

TABLE I  
MAPPING RULE FOR THE FIRST SUB-BLOCK ( $g=1$ ),  $q=2$ ,  $p_1=1$ ,  $p_2=1$ .

Modulated bit	Polarity converter	Carrier Index bit	Time Index bit	Inex of active subcarrier $(\gamma_f, \gamma_t)_v^g$	$D^g$	$(f_i, t_j)^*$
0	-1	0	0	1,1	$\begin{bmatrix} -1 & 0 \\ 0 & 0 \end{bmatrix}$	$(f_1, t_1)$
0	-1	0	1	1,2	$\begin{bmatrix} 0 & -1 \\ 0 & 0 \end{bmatrix}$	$(f_1, t_2)$
0	-1	1	0	2,1	$\begin{bmatrix} 0 & 0 \\ -1 & 0 \end{bmatrix}$	$(f_2, t_1)$
0	-1	1	1	2,2	$\begin{bmatrix} 0 & 0 \\ 0 & -1 \end{bmatrix}$	$(f_2, t_2)$
1	1	0	0	1,1	$\begin{bmatrix} 1 & 0 \\ 0 & 0 \end{bmatrix}$	$(f_1, t_1)$
1	1	0	1	1,2	$\begin{bmatrix} 0 & 1 \\ 0 & 0 \end{bmatrix}$	$(f_1, t_2)$
1	1	1	0	2,1	$\begin{bmatrix} 0 & 0 \\ 1 & 0 \end{bmatrix}$	$(f_2, t_1)$
1	1	1	1	2,2	$\begin{bmatrix} 0 & 0 \\ 0 & 1 \end{bmatrix}$	$(f_2, t_2)$

\*  $f_i$  SELECTED FREQUENCY FOR THE  $g^{th}$  GROUP,  $t_j$  SELECTED TIME FOR THE  $g^{th}$

The total number of available subcarriers is  $(2^q + 1)$ ,  $q$  represents an integer value,  $p_1 \leq q$ , among that one, transmits the reference chaotic signal; the rest of the bits are grouped into  $L$  sets, with each set containing  $2^{p_1}$  subcarriers, i.e.  $L = 2^{q-p_1}$ . In each  $g^{th}$  group, The carrier index bits are carried by one subcarrier out of  $N$ . The total number of bits utilized for carrier indexing is  $p_1 = \log_2 N$ . In a similar manner, one of the  $Q$  time slots is assigned for transmitting the time index bits. Consequently, the amount of time index bits equals  $p_2 = \log_2 Q$ . The last bits of  $S_v$  are modulated with DCSK over the active subcarrier.

Through the utilization of the index selector,  $p_1$  bits that represent carrier indices are linked to the carrier index sequence denoted as  $w = [w_1, w_2, \dots, w_q, \dots, w_N]$ , in this sequence, when  $w_q = 1$ , it signifies the selection of the  $q^{th}$  subcarrier, while  $w_q = 0$  indicates the exclusion of the  $q^{th}$  subcarrier. Moreover, the time index sequence can be denoted as  $u = [u_1, u_2, \dots, u_t, \dots, u_Q]$ , with  $u_t = 1$  indicating the selection of the  $t^{th}$  time slot, while  $u_t = 0$  signifies the non-selection of the  $t^{th}$  time slot. In particular, let's assume that  $\gamma_f$  and  $\gamma_t$  are two modulation symbols for position indexing, where they can be calculated by the carrier index bits and the time index bits, respectively. Consequently, the carrier index sequence and time index sequence are obtained  $[w_1, w_2, \dots, w_N] = [0, 0, \dots, 1_{\gamma_f}, \dots, 0]$  and  $[u_1, u_2, \dots, u_Q] = [0, 0, \dots, 1_{\gamma_t}, \dots, 0]$ , respectively.

Within each sub-block, the indexed bits,  $p_1$  and  $p_2$ , are converted to index symbols. In this specific sub-block, one subcarrier and one time slot are chosen, leading to the creation of sequences represented as  $d_{v,i,j}^g$ , where,  $1 \leq i \leq N$ ,  $1 \leq j \leq Q$ ,  $g = 1, \dots, L$ . The value of  $d_{v,i,j}^g$  is decided by the  $g^{th}$  modulated bits ( $b^g$ ) when  $i = \gamma_f$  and  $j = \gamma_t$ , where  $d_{v,i,j}^g$  can take values of either +1 or -1. Otherwise, it equals 0. Consequently, within each sub-block, there exists only a single non-zero coefficient among the  $2^{p_1}$  coefficients.

A simple mapping rule is shown in Table I for  $q=2$ ,  $p_1=1$ ,

and  $p_2=1$ . There are two sub-blocks ( $L=2$ ), and four coefficients are present in every sub-block  $d_{(i,j)}^g \in D^g$ ,  $D^g \in \mathbb{R}^{N \times Q}$ ,  $i = 1, 2$ ,  $j = 1, 2$ ,  $g = 1, 2$ . This table also shows the active frequencies and time slots within each sub-block, i.e. for sub-blocks 1 and 2, the patterns  $f_1 f_2 t_1 t_2 f_3 f_4 t_1 t_2$  are utilized, respectively.

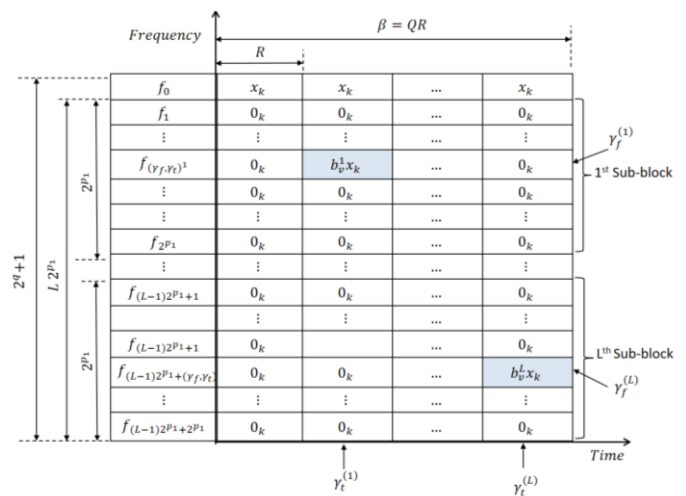


Fig. 2. Format of the signal transmitted by GFTIM-DCSK-I system. \*Where  $0_k =$  zero vector with length  $R$ ,  $x_k = [x_1, x_2, \dots, x_R]$ .

During the duration of the  $v^{th}$  symbol, the reference chaotic sequence undergoes a pulse-shaping filter process with a spreading factor of length  $R$  in accordance with the formula:

$$x_v(t) = \sum_{k=1}^R x_{v,k} y(t - kT_c) \quad (1)$$

Within this scheme, the reference chaotic sequence, denoted as  $x_v(t)$ , is sent by the initial subcarrier with a center frequency of  $f_0$ , where  $y(t)$  represents the square-root-raised cosine filter and  $T_c$  is the chip time. During the  $v^{th}$  symbol interval, the total transmitted signal may be described as:

$$s(t) = \sum_{g=1}^L \sum_{i=1}^{2^{p_1}} b^g c_{i,n}^g \cos(2\pi f_{(g-1)2^{p_1}+i} t +$$

$$\phi_{(g-1)2^{p_1+i}}) + x_v(t)\cos(2\pi f_0 t + \phi_0) \quad (2)$$

$$c_{i,n} = [c_{i,1,k}, c_{i,2,k}, \dots, c_{i,2^{p_2},k}] \quad (3)$$

$$c_{i,j,k} = \begin{cases} x_k & j = \gamma_t \\ 0 & \text{otherwise} \end{cases} \quad (4)$$

The  $f_{(g-1)2^{p_1+i}}$  and  $\phi_{(g-1)2^{p_1+i}}$  represent the center frequency and phase angle of the  $i^{\text{th}}$  subcarrier in the  $g^{\text{th}}$  sub-block, respectively.

Fig. 2 illustrates the structure of the transmission signal utilized in the GFTIM-DCSK-I system. The frequency domain is represented by the vertical axis, and the time domain is represented by the horizontal axis.

### B. Receiver

Fig. 3 illustrates the receiver of the proposed GFTIM-DCSK-I system. The channel model for multipath Rayleigh fading channel is defined as [41]  $\eta(t) = \sum_{l=1}^P \lambda_l \delta(t - \tau_l)$ , where  $P$  is the number of paths and  $\tau_l$ ,  $\lambda_l$  is the path delay of the  $l^{\text{th}}$  path and the channel coefficient, respectively. The channel coefficients  $\lambda_l$  in this study are taken to be independent random variables with a Rayleigh distribution. The channel's received signal output may be expressed as:

$$r(t) = s(t) * \eta(t) + n(t) \quad (5)$$

where the symbol  $*$  represents the convolution function, while  $n(t)$  denotes the wideband AWGN signal with a zero mean and a power spectral density of  $N_0/2$ . Furthermore, the corresponding orthogonal carrier frequencies may be used to separate the received signals, which are further filtered using a set of matching filters. The demodulated discrete outputs consist of two components: the reference-chaotic signals and the information-bearing signals. The reference chaotic signals are denoted with a matrix  $A$  of size  $1 \times \beta$ , where  $\beta$  is defined

of the  $g^{\text{th}}$  sub-block are represented by another matrix  $B^g$  with dimensions  $R \times (NQ)$ , where  $g$  ranges from 1 to  $L$ .

$$B^g = [B_1 B_2 B_3, \dots, B_N], B_i \in \mathbb{R}^{R \times N} \quad (6)$$

where

$$B_i = \begin{bmatrix} d_i c_{i,1,1} & d_i c_{i,2,1} & \dots & d_i c_{i,2^{p_2},1} \\ d_i c_{i,1,2} & d_i c_{i,2,2} & \dots & d_i c_{i,2^{p_2},2} \\ \vdots & \vdots & \ddots & \vdots \\ d_i c_{i,1,R} & d_i c_{i,2,R} & \dots & d_i c_{i,2^{p_2},R} \end{bmatrix}, 1 \leq i \leq N \quad (7)$$

An average and summation are applied to the received reference-chaotic signals. The averaged reference-chaotic signal is then utilized to demodulate the information-carrying signals. As a result, the average reference chaotic signal is represented as:

$$\tilde{x}_{avg,k} = \frac{1}{Q} \sum_{j=1}^Q \sum_{l=1}^P \lambda_l x_{j,k-\tau_l} + n_j^k \quad (8)$$

$$\tilde{n}_k = \frac{1}{Q} \sum_{j=1}^Q n_j^k \quad (9)$$

After this, we compute the  $v^{\text{th}}$  symbol and  $g^{\text{th}}$  group correlation matrices  $Z_v^g$ , where  $g$  ranges from 1 to  $L$ , and each matrix has dimension  $1 \times (NQ)$ .

$$Z_v^g = \tilde{x}_{avg,k}^T \times B^g = [z_{v,1}^g z_{v,2}^g \dots z_{v,2^{p_1+p_2}}^g]^T, g=1, \dots, L \quad (10)$$

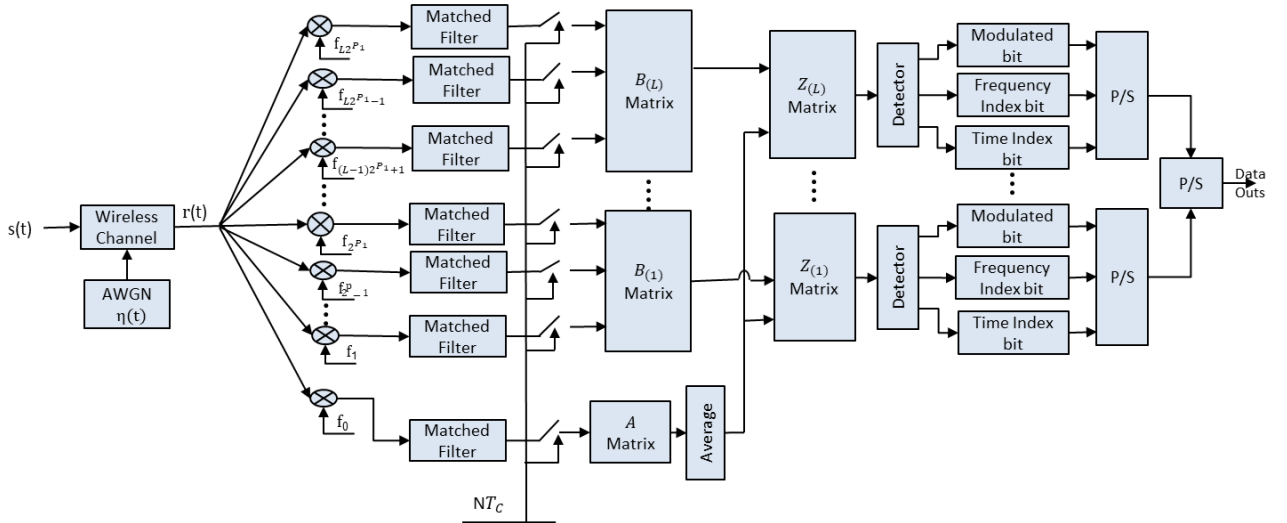


Fig. 3. The structure of the receiver for the GFTIM-DCSK-I system.

as  $\beta = QR$ . On the other hand, the information-bearing signals

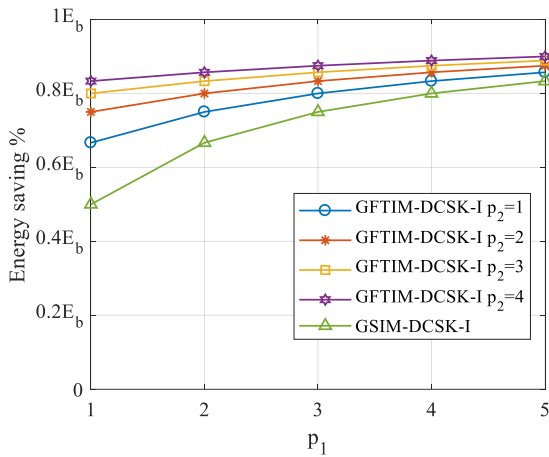


Fig. 4. Comparisons of Energy saving versus  $p_1$  values for GSTIM-DCSK-I with various techniques at  $p_2=1,2,3,4$  and  $q=8$ .

TABLE III  
SPECTRAL EFFICIENCY COMPARED WITH SEVERAL DCSK MODULATIONS.

Modulation	Spectral Efficiency
DCSK	$1/\beta T_c B$
MC-DCSK [8],[24]	$M/(M+1) \beta T_c B$
CI-DCSK1 [33]	$(q+1)/((M+1) \beta T_c B)$
2CI-DCSK [35]	$(2q+2)/((M+1) \beta T_c B)$
GSIM-DCSK-I [42]	$M(p_1 + 1)/(2^{p_1} (M+1) \beta T_c B)$
GFTIM-DCSK-I	$M(p_1 + p_2 + 1)/(2^{p_1} (M+1) \beta T_c B)$

The maximum absolute value of  $Z_{v,\rho}^g$  for  $\rho=1, \dots, 2^{p_1+p_2}$  is used to determine the active subcarrier and time index within the  $g^{\text{th}}$  sub-block, and it may be represented as:

$$(\tilde{Y}_f, \tilde{Y}_t)_v^g = \arg \max_{\substack{i=1, \dots, N \\ j=1, \dots, Q}} (|z_v^g(i, j)|), \quad g = 1, \dots, L \quad (11)$$

where  $(\tilde{Y}_f, \tilde{Y}_t)_v^g$  represents the active subcarrier's predicted carrier and time index in the  $g^{\text{th}}$  sub-block. Using Table I in reverse mapping, the index bits estimated for the  $g^{\text{th}}$  sub-block are computed by converting  $(\tilde{Y}_f, \tilde{Y}_t)_v^g$  into a binary number, i.e.  $[\hat{a}_{v,(g-1)p+p_1+p_2}, \dots, \hat{a}_{v,(g-1)p+p_1+p_2+1}] = \text{Reverse-Mapping}((\tilde{Y}_f, \tilde{Y}_t)_v^g)$ ,  $g = 1, \dots, L$ . In the  $g^{\text{th}}$  sub-block, the recovered modulated bit is estimated via:

$$\hat{a}_{v,(g-1)p+p_1+p_2+1} = \begin{cases} 0 & \text{if } \text{sign}(z_{v,\tilde{Y}_f,\tilde{Y}_t}^g) = -1 \\ 1 & \text{if } \text{sign}(z_{v,\tilde{Y}_f,\tilde{Y}_t}^g) = +1 \end{cases}, \quad g = 1, \dots, L \quad (12)$$

#### IV. SYSTEM ANALYSIS

##### A. Energy Efficiency

In GFTIM-DCSK-I systems,  $L(p_1 + p_2)$  bits are transmitted in selecting times and subcarriers, whereas only one bit out of

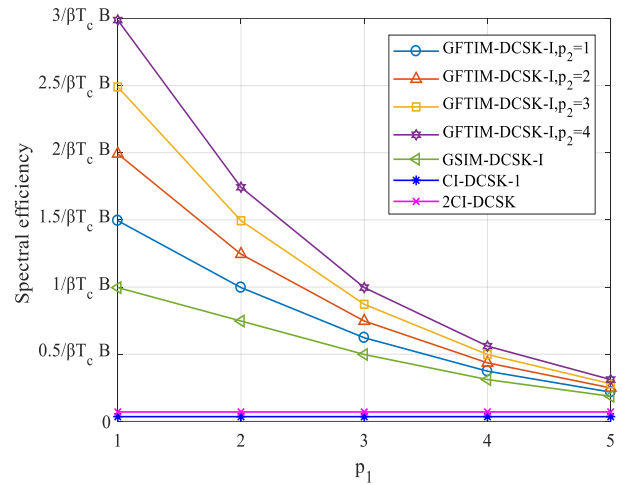


Fig. 5. Comparisons of spectral efficiency versus  $p_1$  values for GFTIM-DCSK-I with various techniques at  $p_2=1,2,3,4$  and  $q=8$ .

the total  $Lp$  is directly modulated using DCSK modulation. Since the transmission energy of each modulated bit is equal to  $E_b$ , mapping to index subcarriers and index times should decrease the total energy needed for transmission. The energy saving depends on the ratio of the number of subcarriers and time slots used for indexing to the system's modulation order. Hence, in the suggested scheme, the percentage of energy savings per block is specified by [36]:

TABLE II  
ENERGY SAVING COMPARISON FOR DIFFERENT DCSK MODULATIONS.

Modulation	$E_{\text{saving}}$
CI-DCSK1	$(1 - (1/(q+1)))E_b\%$
GSIM-DCSK-I	$(1 - (1/(p_1+1)))E_b\%$
GFTIM-DCSK-I	$(1 - (1/(p_1+p_2+1)))E_b\%$

$$E_{\text{saving}} = \left(1 - \frac{1}{(p_1+p_2+1)}\right) E_b\% \quad (13)$$

From Fig. 4, it's clear that the GFTIM-DCSK-I system saves more energy when the number of bits of subcarriers or times indices is increased. Nevertheless, the spectral efficiency decreases as the number of subcarriers augments, so it is better to index via times because it leads to lower energy and spectral efficiency costs. The energy-saving comparison for several DCSK modulations is displayed in Table II.

##### B. Spectral Efficiency

The bit rate to total bandwidth ratio is the definition of spectral efficiency [35], [6]. Assuming that the bandwidth for each subcarrier is the same and denoted as  $B$ , the spectral efficiency of GFTIM-DCSK-I, represented as  $\eta_{\text{GFTIM-DCSK-I}}$ , may be mathematically represented as follows:

$$\eta_{\text{GFTIM-DCSK-I}} = \frac{\text{bit rate}}{\text{total bandwidth}} = \frac{L(p_1+p_2+1)}{\beta T_c} = \frac{L(p_1+p_2+1)}{(2^q+1)\beta T_c B} \quad (14)$$

Table III presents a comparative analysis of spectral

efficiency among several DCSK modulation techniques. The variables  $M$  and  $p_1$  are used to represent the spectral efficiency of the GFTIM-DCSK-I system, where  $L=M/2^{p_1}$ . From this table, it's clear that the MC-DCSK has a higher spectral efficiency. The spectral efficiency of GFTIM-DCSK-I in comparison to other DCSK modulations is illustrated in Fig. 5. It is evident from this figure that GFTIM-DCSK-I outperforms CI-DCSK1, 2CI-DCSK, and GSIM-DCSK-I in terms of spectral efficiency, and that its performance increases with an increase in  $p_2$ . The reason for this is that while using the same bandwidth, spectral efficiency is proportional to the rate of data transmission.

### C. Complexity Analysis

All systems are assumed to have the same total number of subcarriers, which equals  $(2^q+1)$ . For GFTIM-DCSK-I, GSIM-DCSK-I, CI-DCSK1, 2CI-DCSK, and MC-DCSK techniques, the total bits that are conveyed per symbol duration are  $L(p_1+p_2+1)$ ,  $2^{q-p_1}(p_1+1)$ ,  $(q+1)$ ,  $2(q+1)$ , and  $2^q$ , respectively. The primary determinant of hardware complexity when comparing DCSK modulations is the number of multiplications executed during the spreading/despreading process for each bit throughout one symbol's duration. Hence, the whole focus lies on the multiplication that takes place between the modulated bits and the chaotic signal at the transmitting side, as well as the multiplication that takes place at the energy detector on the receiving side, where the chaotic information signal is multiplied by the reference chaotic signal. For CI-DCSK1, 2CI-DCSK, MC-DCSK, GSIM-DCSK-I, and GFTIM-DCSK-I, the overall number of multiplications per bit through one symbol period may be represented as follows [42]:

$$O_{CI-DCSK1} = \frac{(2^q\beta+2^q\beta)}{(q+1)} = \frac{2^{q+1}}{(q+1)}\beta \quad (15)$$

$$O_{2CI-DCSK} = \frac{(2^{q+1}\beta+2^{q+1}\beta)}{2(q+1)} = \frac{2^{q+1}}{(q+1)}\beta \quad (16)$$

$$O_{MC-DCSK} = \frac{(2^q\beta+2^q\beta)}{2^q} = 2\beta \quad (17)$$

$$O_{GSIM-DCSK-I} = \frac{(2^q\beta+2^q\beta)}{2^{(q-p_1)}(p_1+1)} = \frac{2^{p_1+1}}{(p_1+1)}\beta \quad (18)$$

$$O_{GFTIM-DCSK-I} = \frac{(2^q\beta+2^q\beta)}{2^{(q-p_1)}(p_1+p_2+1)} = \frac{2^{p_1+1}}{(p_1+p_2+1)}\beta \quad (19)$$

where equations (15)-(19) represent the multiplication number for one bit during one symbol period for CI-DCSK1, 2CI-DCSK, MC-DCSK, GSIM-DCSK-I, and GFTIM-DCSK-I, respectively. It is evident that the GFTIM-DCSK-I has a multiplication number per one bit during one symbol lower than that of the GSIM-DCSK-I and CI-DCSK1 (2CI-DCSK) but higher than that of the MC-DCSK. On the other hand, GFTIM-DCSK-I's extra complexity has been used to achieve higher data rate, EE, and spectral efficiency than other comparable systems. The components required for evaluating the transmitter and receiver complexity in GFTIM-DCSK-I,

TABLE IV  
COMPARISON OF THE HARDWARE COMPLEXITY FOR SEVERAL DCSK MODULATIONS AT THE TRANSMITTING END.

Component	CI-DCSK	2CI-DCSK	MC-DCSK	GSIM-DCSK	GFTIM-DCSK-I
Adder	1	$2^{q+1}$	1	1	1
Multipliers	$2^{q+1}+1$	$3.2^{q+1}$	$2^{q+1}+1$	$2^{q+1}+1$	$2^{q+1}+1$
Index mappers/Selector	1	2	1	$L$	$2L$
Pulse shaping filter	1	2	1	1	1
Hilbert filter	0	1	0	0	0

TABLE V  
COMPARISON OF THE HARDWARE COMPLEXITY FOR VARIOUS DCSK MODULATIONS AT THE RECEIVING END.

Component	CI-DCSK	2CI-DCSK	MC-DCSK	GSIM-DCSK	GFTIM-DCSK-I
Multiplier	$2^{q+1}$	$2^{q+1}$	$2^{q+1}$	$2^{q+1}$	$2^{q+1}$
Matched filter	$2^{q+1}$	$2^{q+1}$	$2^{q+1}$	$2^{q+1}$	$2^{q+1}$
Energy detector	$2^q$	$2^{q+1}$	$2^q$	$2^q$	$2^{q+p_2}$
Hilbert filter	0	1	0	0	0

GSIM-DCSK-I, CI-DCSK, 2CI-DCSK, and MC-DCSK are shown in Tables IV and V, respectively.

### V. ANALYSIS OF BER PERFORMANCE

In order to simplify the analysis of BER, it is assumed that the maximum multipath delay is much shorter than the symbol duration, specifically denoted as  $0 < \tau_{max} \ll R$ . Hence, the study does not take into account the phenomenon of inter-symbol interference (ISI) [26], [33], [42]. Additionally, it may be assumed that the channel has a slow Rayleigh fading effect, with the coefficients remaining constant for one symbol period.

In the GFTIM-DCSK-I system, inside each sub-block, there is only one active subcarrier, whereas the number of inactive subcarriers is determined by the formula  $(2^{p_1}-1)$ . For all sub-blocks, the total bits sent are  $L(p_1+p_2+1)$ . Thus, at the  $v^{th}$  symbol period, the decision variables for the active subcarrier at the correlator output are  $Z_{v,i,j}^g, 1 \leq g \leq L, i = \gamma_f, j = \gamma_t$ , while for the  $i^{th}$  inactive subcarrier, they are  $Z_{v,i,j}^g, 1 \leq g \leq L, 1 < i \leq 2^{p_1}, 1 < j \leq 2^{p_2}$ , where  $i \neq \gamma_f, j \neq \gamma_t$ . Since no data is being sent across the idle subcarriers, in this instance, just

noise is being received.

Therefore if  $i = \gamma_f$  and  $j = \gamma_t$ , the element of matrix  $Z$  is given by:

$$Z_{v,\gamma_f,\gamma_t}^g = \sum_{k=1}^R \left( \sum_{l=1}^P \alpha_{v,l} x_{v,k-\tau_l} d_{v,i,j}^g + n_{v,\gamma_f,\gamma_t}^{(k)} \right) \times \left( \sum_{l=1}^P \alpha_{v,l} x_{v,k-\tau_l} + \tilde{n}_{v,k} \right), \quad g = 1, \dots, L \quad (20)$$

If  $i \neq \gamma_f$  and  $j \neq \gamma_t$ , then the element of matrix  $Z$  is:

$$Z_{v,i,j}^g = \sum_{k=1}^R \left( \sum_{l=1}^P \alpha_{v,l} x_{v,k-\tau_l} + \tilde{n}_{v,k} \right) n_{v,i,j}^{(k)}, \quad g = 1, \dots, L \quad (21)$$

The variables  $n_{v,\gamma_f,\gamma_t}^{(k)}$ ,  $n_{v,i,j}^{(k)}$  and  $\tilde{n}_{v,k}$  represent Gaussian noise associated with the active subcarrier, the inactive subcarrier, and the reference subcarrier, respectively. The  $n_{v,\gamma_f,\gamma_t}^{(k)}$  and  $n_{v,i,j}^{(k)}$  have the same means and variances.

The equation that follows can be used for large values of  $R$  [33], [35]:

$$\sum_{k=1}^R x_{k-\tau_l} x_{k-\tau_u} \approx 0, \quad l \neq u \quad (22)$$

Considering that every sub-block is the same, just the first one is taken into account. The approximations for the means and variances of  $Z_{v,i,j}$  are as follows:

$$E(Z_{v,i,j}) = \begin{cases} \sum_{l=1}^P \alpha_{v,l}^2 \sum_{k=1}^R x_{v,k}^2 d_{v,i,j}^1, & i = \gamma_f, j = \gamma_t \\ 0, & 1 < i \leq 2^{p_1}, 1 < j \leq 2^{p_2}, \\ & \text{where } i \neq \gamma_f, j \neq \gamma_t \end{cases} \quad (23)$$

$$V(Z_{v,i,j}) = \begin{cases} \sum_{l=1}^P \alpha_{v,l}^2 \sum_{k=1}^R x_{v,k}^2 \frac{N_0}{2} + \sum_{l=1}^P \alpha_{v,l}^2 \sum_{k=1}^R x_{v,k}^2 \frac{N_0}{2Q} \\ \quad + \frac{RN_0^2}{4Q}, \text{ where } i = \gamma_f, j = \gamma_t \\ \frac{1}{2} \sum_{l=1}^P \alpha_{v,l}^2 \sum_{k=1}^R x_{v,k}^2 N_0 + \frac{RN_0^2}{4Q}, \\ 1 < i \leq 2^{p_1}, 1 < j \leq 2^{p_2}, \text{ where } i \neq \gamma_f, j \neq \gamma_t \end{cases} \quad (24)$$

The functions  $E(\cdot)$  and  $V(\cdot)$  represent the mean and variance functions, respectively. Describe GFTIM-DCSK-I bit energy

as  $E_b = \frac{(L+Q) \sum_{k=1}^R x_{v,k}^2}{L(p_1+p_2+1)}$ , as well as the bit signal-to-noise ratio  $\gamma_b = \frac{E_b \sum_{l=1}^P \alpha_{v,l}^2}{N_0}$ . Equations (23) and (24) may be reformulated in terms of the parameter  $\gamma_b$ , yielding the following expressions:

$$E(Z_{v,j}) = \begin{cases} N_0 \frac{L(p_1+p_2+1)\gamma_b}{(L+Q)} = \mu_1, & i = \gamma_f, j = \gamma_t \\ 0 = \mu_2, & 1 < i \leq 2^{p_1}, 1 < j \leq 2^{p_2} \\ & \text{where } i \neq \gamma_f, j \neq \gamma_t \end{cases} \quad (25)$$

$$V(Z_{v,i,j}) = \begin{cases} \frac{N_0^2}{2} \left( \frac{L(p_1+p_2+1)\gamma_b}{(L+Q)} + \frac{L(p_1+p_2+1)\gamma_b}{Q(L+Q)} + \frac{R}{2Q} \right) = \sigma_1^2, & i = \gamma_f, j = \gamma_t \\ \frac{N_0^2}{2} \left( \frac{L(p_1+p_2+1)\gamma_b}{(L+Q)} + \frac{R}{2Q} \right) = \sigma_2^2, & 1 < i \leq 2^{p_1}, 1 < j \leq 2^{p_2}, \text{ where } i \neq \gamma_f, j \neq \gamma_t \end{cases} \quad (26)$$

The theoretical BER of GFTIM-DCSK-I,  $P_{BER-I}$  may be expressed as the sum of two components: the BER of the index bits,  $P_{index-I}$ , and the BER of the modulated bits,  $P_{mod-I}$ . Since each sub-block has one bit for modulated bits and  $p_1+p_2$  bits for indices bits,  $P_{BER-I}$  may be written as follows:

$$P_{BER-I} = \frac{1}{p_1+p_2+1} P_{mod-I} + \frac{p_1+p_2}{p_1+p_2+1} P_{index-I} \quad (27)$$

1) *The BER of the index bits ( $P_{index-I}$ ):* If the decision variable's absolute value for the correct subcarrier index  $Z_{v,\gamma_f,\gamma_t}$  is less than the maximum absolute value for an incorrect subcarrier index  $|Z_{v,i,j}|$ ,  $1 < i \leq 2^{p_1}$ ,  $1 < j \leq 2^{p_2}$ , an error will occur. For index bits the formulation of the symbol error rate (SER)  $P_{SER-index-I}$  is expressed by [33], [35], [44], [42]:

$$P_{SER-index-I} = Pr \left[ |Z_{v,\gamma_f,\gamma_t}| < \max(|Z_{v,i,j}|) \right] = 1 - \int_0^{+\infty} \left( F_{|Z_{v,i,j}|}(y, \mu_2, \sigma_2^2) \right)^{2^{p_1} 2^{p_2-1}} f_{|Z_{v,\gamma_f,\gamma_t}|}(y, \mu_1, \sigma_1^2) dy \quad (28)$$

where  $F_{|Z_{v,i,j}|}(y, \mu_2, \sigma_2^2)$  the cumulative distribution function (CDF) of  $|Z_{v,i,j}|$ ,  $1 < i \leq 2^{p_1}$ ,  $1 < j \leq 2^{p_2}$ , and  $f_{|Z_{v,\gamma_f,\gamma_t}|}(y, \mu_1, \sigma_1^2)$  the probability density function (PDF) of  $|Z_{v,\gamma_f,\gamma_t}|$ , are flowed folded normal distribution and can be determined from [33], [35]:

$$F_{|Z_{v,i,j}|}(y, \mu_2, \sigma_2^2) = erf \left( \frac{y-\mu_2}{\sqrt{2\sigma_2^2}} \right) \quad (29)$$

$$f_{|Z_{v,\gamma_f,\gamma_t}|}(y, \mu_1, \sigma_1^2) = \frac{1}{\sqrt{2\pi\sigma_1^2}} \left( e^{-\frac{(y-\mu_1)^2}{2\sigma_1^2}} + e^{-\frac{(y+\mu_1)^2}{2\sigma_1^2}} \right) \quad (30)$$

By substituting equations (25), (26), (29), and (30) into equation (28), the expression for  $P_{SER-index-I}$  may be determined as:

$$P_{SER-index-I} = 1 - \frac{2Q(L+Q)}{\sqrt{\pi N_0^2 (2LQ(2^{p_1} 2^{p_2-1})\gamma_b + 2L(p_1+p_2+1)\gamma_b + 2R(L+Q))}} \quad (31)$$

$$\int_0^{+\infty} \left( \operatorname{erf} \left( \frac{\sqrt{2Q(L+Q)}y}{\sqrt{N_0^2(2Q(p_1+p_2+1)\gamma_b+R(L+Q))}} \right) \right)^{2^{p_1} 2^{p_2-1}} \left( \exp \left( -\frac{2Q((L+Q)y-N_0 L(p_1+p_2+1)\gamma_b)^2}{N_0^2(L+1)(2QL(p_1+p_2+1)\gamma_b+2L(p_1+p_2+1)\gamma_b+R(L+Q))} \right) + \exp \left( -\frac{2Q((L+Q)y+N_0 L(p_1+p_2+1)\gamma_b)^2}{N_0^2(L+1)(2QL(p_1+p_2+1)\gamma_b+2L(p_1+p_2+1)\gamma_b+R(L+Q))} \right) \right) dy \quad (31)$$

$P_{index-I}$ , which is dependent upon  $P_{SER-index-I}$ , may be obtained as follows [44], [46]:

$$P_{index-I} = \frac{2^{(p_1+p_2+1)}}{2^{p_1} 2^{p_2-1}} P_{SER-index-I} \quad (32)$$

2) *BER for Modulated Bits ( $P_{mod-I}$ ):* There are two scenarios that lead to the modulated bit errors. One where there is an error in the modulated bits but not in the subcarrier-time index bits. In this instance, the BER of the modulated bits  $P_{DCSK-I}$  is computed as follows:

$$P_{DCSK-I} = \frac{1}{2} \operatorname{erfc} \left[ \left( \frac{2\sigma_1^2}{\mu_1^2} \right)^{\frac{1}{2}} \right] = \frac{1}{2} \operatorname{erfc} \left[ \left( \frac{(L+Q)}{L(p_1+p_2+1)\gamma_b} + \frac{(L+Q)}{LQ(p_1+p_2+1)\gamma_b} + \frac{R}{2Q L^2(p_1+p_2+1)^2(\gamma_b)^2} \right)^{\frac{1}{2}} \right] \quad (33)$$

In the second scenario, when the subcarrier-time index bits are incorrect, the modulated bits are recovered from the incorrect correlator, resulting in a 0.5 detection probability. The representation of  $P_{mod-I}$  may be derived from analyzing the two situations:

$$P_{mod-I} = P_{DCSK-I}(1 - P_{SER-index-I}) + 0.5P_{SER-index-I} \quad (34)$$

By substituting equations (32) and (34) into equation (27), we can extract the expression for the  $P_{BER-I}$  over a multipath Rayleigh fading channel.

The average BER for GFTIM-DCSK-I through a multipath fading channel is obtained by integrating the probability of BER ( $P_{BER-I}$ ) over  $\gamma_b$ :

$$P_{Rayleigh} = \int_0^{+\infty} P_{BER-I} f(\gamma_b) d\gamma_b \quad (35)$$

where  $f(\gamma_b)$  is the PDF of  $\gamma_b$ , may be represented as [33], [35]:

$$f(\gamma_b) = \frac{(\gamma_b)^{L-1}}{(L-1)! (\bar{\gamma}_b)^L} \exp \left( -\frac{\gamma_b}{\bar{\gamma}_b} \right) \quad (36)$$

$$\text{where } \bar{\gamma}_b = \frac{E_b \sum_l^P E(\alpha_{v,l}^2)}{N_0} \quad (37)$$

By substituting  $P = 1$ ,  $\tau_1 = 0$ , and  $\alpha_{v,1} = 1$  in each equation, the aforementioned formulas may also be used to derive the BER theory of GFTIM-DCSK-I under AWGN.

## VI. NUMERICAL RESULTS AND DISCUSSION

This section presents an evaluation of the theoretical and simulated BER performance of the proposed system: multipath Rayleigh fading and additive white Gaussian noise (AWGN). The following parameters are established for a multipath Rayleigh fading channel: the fading path  $P = 2$ , the same average power gains  $E(\alpha_1^2) = E(\alpha_2^2) = \frac{1}{3}$ , and the paths  $\tau_1=0$  and  $\tau_2=2$ .

### A. Evaluation of Performance

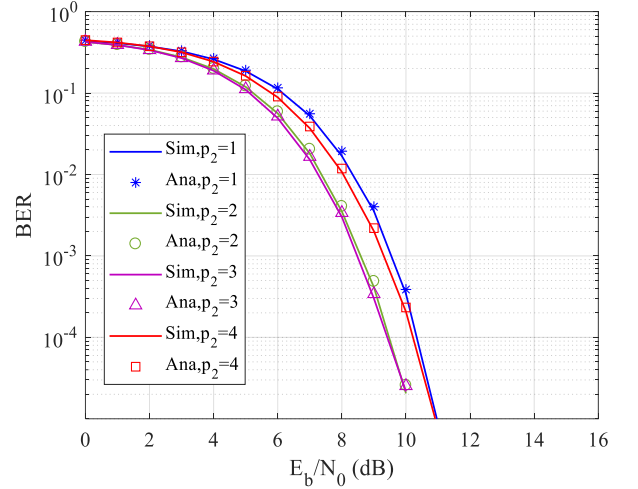


Fig. 6. BER against  $E_b/N_0$  for GSTIM-DCSK-I system in AWGN channel with  $R=128$ ,  $q=5$ ,  $p_1=2$ ,  $p_2=1,2,3,4$ .

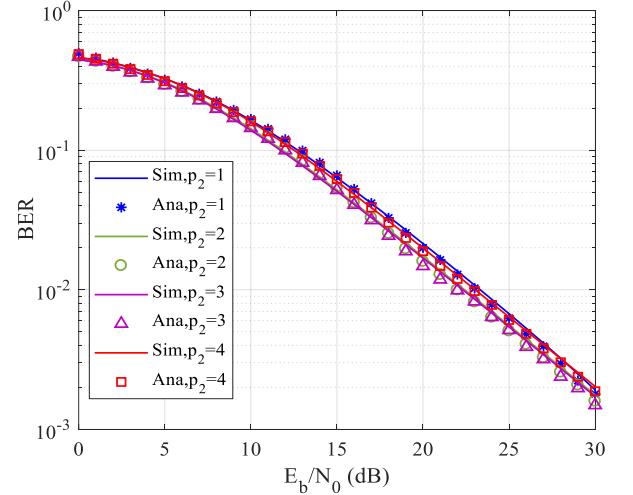


Fig. 7. BER against  $E_b/N_0$  for GSTIM-DCSK-I system in Rayleigh fading channel with  $R=128$ ,  $q=5$ ,  $p_1=2$ ,  $p_2=1,2,3,4$ .

The GFTIM-DCSK-I system utilizes a total of 33 subcarriers and mapped bits, with the carrier index and time index denoted as  $q=5$ ,  $p_1=1,2,3,4$ , and  $p_2=1,2,3,4$ , respectively. These specific parameters are chosen to assess the performance of the system in terms of BER. The analysis involves comparing the analytical and simulated BER of the GFTIM-DCSK-I system, considering the presence of AWGN and multipath Rayleigh fading channels with a parameter  $R=128$  as illustrated in Figures 6 and 7, respectively. The

impact of varying  $p_2$  values on this system's BER performance is depicted in these figures. The results of the simulation exhibit a high degree of concordance with the theoretical BER expressions, therefore confirming the precision of our theoretical study. These Figures indicate that while  $p_1$  remains constant, degradation of the system's BER performance will occur with an increase in  $p_2$ . Also, the BERs of the multipath fading channel are slightly changed by changing the  $p_2$  value.

The impact of increasing  $p_1$  on the GFTIM-DCSK-I system's BER performance in the AWGN channel is shown in Fig. 8. This Figure makes it evident that increasing  $p_1$  while keeping  $p_2$  at a fixed value results in a bit of deterioration in system performance at  $p_1=1$  or 2 but this deterioration increased as the value of  $p_1$  increase, for instance, with a BER level equal to  $10^{-4}$ , the SNR gain for  $p_1=3$  is 1dB less than that of  $p_1=1$ , where the total bits for  $p_1=1,3$  and  $p_2=2$  are 64 and 24 bits, respectively. Moreover, Fig. 9 shows this effect under Rayleigh fading channel. A slight increase in BER is observed when the value of  $p_1$  is increased.

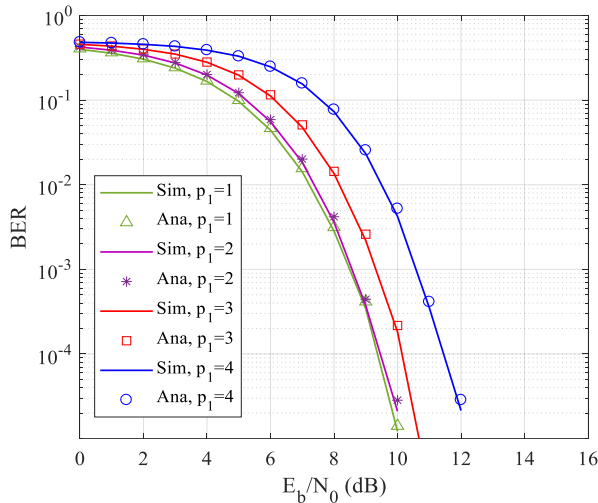


Fig. 8. BER against  $E_b/N_0$  for GFTIM-DCSK-I system in AWGN channel with  $R=128$ ,  $q=5$ ,  $p_2=2$ ,  $p_1=1,2,3, 4$ .

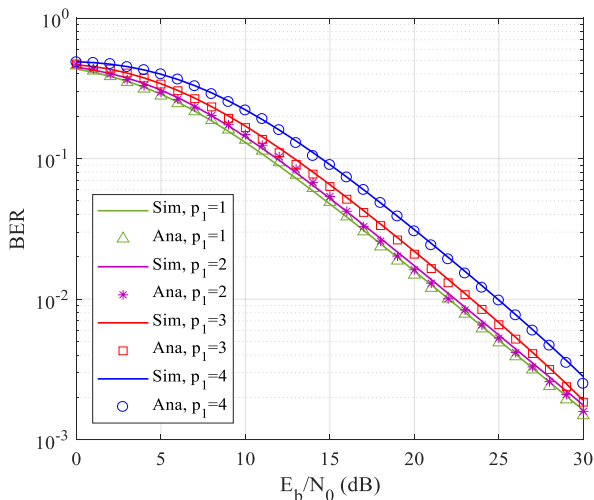


Fig. 9. BER against  $E_b/N_0$  for GFTIM-DCSK-I system in Rayleigh fading channel with  $R=128$ ,  $q=5$ ,  $p_2=2$ ,  $p_1=1,2,3, 4$ .

### B. Comparison with Conventional Index Modulations

Figures 10 and 11 compare the proposed system's BER performance with that of the GSIM-DCSK-I and other DCSK communication systems in the presence of two pathways Rayleigh fading channel and AWGN. The comparison is done by using an equal number of subcarriers. In every modulation scheme, the number of subcarriers is constant at 33 ( $q=5$ ), and for comparison, The carrier and time index bits (mapped bits) are set to  $p_1=2,3$  and  $p_2=2,3$  with  $\beta = 128$ . The total bits sent for the period of each symbol is 24, 40, 24, 16, 6, 32 bits for GFTIM-DCSK-I,  $p_1=3$ ,  $p_2=2$ , GFTIM-DCSK-I,  $p_1=2$ ,  $p_2=2$ , GSIM-DCSK-I with index subcarrier selector bits  $p_1=2$ , GSIM-DCSK-I with index subcarrier selector bits  $p_1=3$ , CI-DCSK1 with total number of available subcarriers ( $q$ )=5, and MC-DCSK, respectively. Fig. 10 clearly shows that the GFTIM-DCSK-I scheme with ( $p_1=3$  and  $p_2=2$ ) and ( $p_1=2$  and  $p_2=2$ ) has better performance over AWGN channel than GSIM-DCSK-I, CI-DCSK1, and MC-DCSK. At BER level  $10^{-3}$ , this system with  $p_1=2$  and  $p_2=2$  gained SNR about 3, 3.25, 3.5, and 4.5 dB higher than the GSIM-DCSK-I,  $p_1=3$ , GSIM-DCSK-I,  $p_1=2$ , and CI-DCSK1, and MC-DCSK system, and this gain will be about 2, 2.25, 2.5, and 4 dB higher than the GSIM-DCSK-I,  $p_1=3$ , GSIM-DCSK-I,  $p_1=2$ , and CI-DCSK1 system with  $p_1=3$ ,  $p_2=2$ , respectively. Additionally, under the influence of fading channels, Fig. 11 compares the BER performance comparisons of GSTIM-DCSK-I for ( $p_1=2$  and  $p_2=2$ ) and ( $p_1=3$  and  $p_2=2$ ) with various DCSK communication systems. This performance is better than that of GSIM-DCSK-I,  $p_1=3$ , GSIM-DCSK-I,  $p_1=2$ , CI-DCSK1, and MC-DCSK modulations.

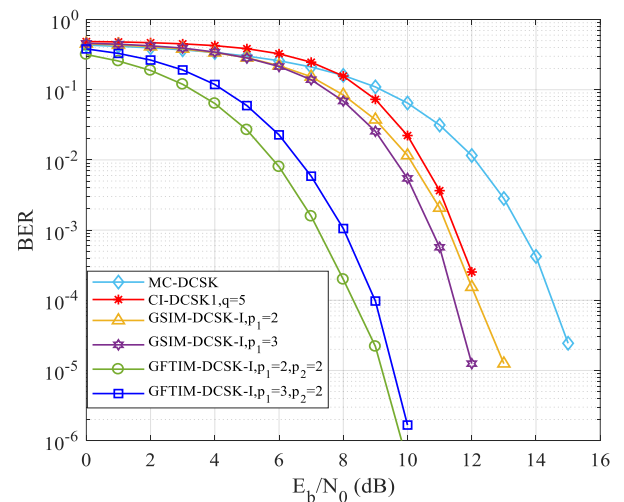


Fig. 10. Comparisons of the BER performance of the proposed GFTIM-DCSK-I and several DCSK techniques over AWGN channel with  $\beta = 128$ ,  $p_1 = 2,3$ , and  $p_2=2$ .

The GFTIM-DCSK-I outperforms the GSIM-DCSK-I, CI-DCSK1, and MC-DCSK systems by around 1, 1.5, and 1.5 dB gain, respectively, at a BER level of  $10^{-2}$ .

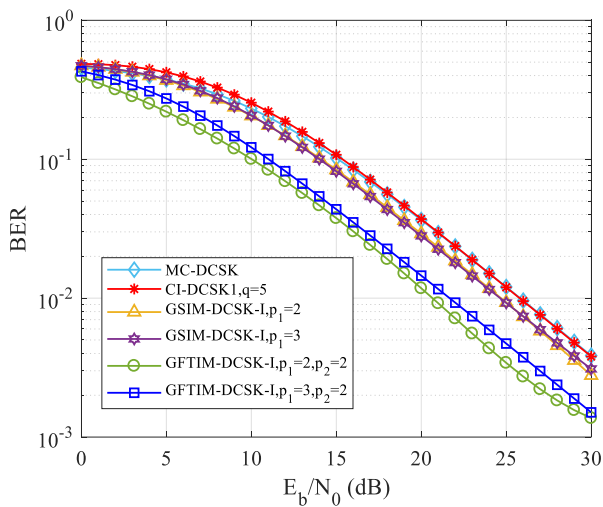


Fig. 11. Comparisons of the BER performance of the proposed GFTIM-DCSK-I and several DCSK techniques over Rayleigh fading channel with  $\beta = 128$ ,  $p_1 = 2, 3$ , and  $p_2 = 2$ .

## VII. CONCLUSION

This study presents a new communication system entitled GFTIM-DCSK-I, which combines time index modulation with GSIM-DCSK modulation. The proposed scheme aims to enhance the spectral efficiency, energy efficiency, and data information rate. By employing this approach, further bits of information may be transmitted through the use of carrier and time indices. In the proposed system, the input bits are partitioned into  $L$  groups, each consisting of  $(p_1 + p_2 + 1)$  bits.  $p_1$  bits are utilized inside each group to choose the active subcarrier. Additionally,  $p_2$  bits are employed to select a specific time slot for the purpose of spreading a modulated bit. The resulting bit is then sent within the active subcarrier. Thus, this system achieves the greatest data rate given that the information bits are transmitted via carrier index bits and time index bits, in addition to modulated bit. The excellent agreement between the simulation results and the analytical BER expressions for AWGN and multipath Rayleigh fading channels gives strong evidence for the high accuracy of the proposed GFTIM-DCSK-I scheme. The comparison of the proposed scheme with existing DCSK schemes like GSIM-DCSK-I, CI-DCSK1, and MC-DCSK for different conditions shows that the proposed system is superior to them in terms of BER performance, energy and spectral efficiency, and data rate in various scenarios. Based on the aforementioned benefits, it can be concluded that the GFTIM-DCSK-I system is a highly promising option for Internet of Things (IoT) applications, including in the domains of Wireless local area network (WLAN) and wireless personal area network (WPAN) with low complexity and power.

## REFERENCES

- [1] G. Kaddoum, "Wireless chaos-based communication systems: A comprehensive survey", *IEEE Access*, vol. 4, pp. 2621-2648, 2016. <https://doi.org/10.1109/access.2016.2572730>
- [2] Y. Tan, W. Xu, T. Huang, and L. Wang, "A multilevel code shifted differential chaos shift keying scheme with code index modulation", *IEEE Transactions on Circuits and Systems II: Express Briefs*, vol. 65, no. 11, pp. 1743-1747, 2017. <https://doi.org/10.1109/tcsii.2017.2764916>
- [3] H.-P. Ren, S.-L. Guo, C. Bai, and X.-H. Zhao, "Cross correction and chaotic shape-forming filter based quadrature multi-carrier differential chaos shift keying communication", *IEEE Transactions on Vehicular Technology*, vol. 70, no. 12, pp. 12675-12690, 2021. <https://doi.org/10.1109/tvt.2021.3119176>
- [4] Y. Tan, W. Xu, T. Huang, and L. Wang, "A multilevel code shifted differential chaos shift keying scheme with code index modulation", *IEEE Transactions on Circuits and Systems II: Express Briefs*, vol. 65, no. 11, pp. 1743-1747, 2017. <https://doi.org/10.1109/tcsii.2017.2764916>
- [5] K. M. Cuomo and A. V. Oppenheim, "Circuit implementation of synchronized chaos with applications to communications", *Physical review letters*, vol. 71, no. 1, p. 65, 1993. <https://doi.org/10.1103/physrevlett.71.65>
- [6] H. Dedieu, M. P. Kennedy, and M. Hasler, "Chaos shift keying: modulation and demodulation of a chaotic carrier using self-synchronizing Chua's circuits", *IEEE Transactions on Circuits and Systems II: Analog and Digital Signal Processing*, vol. 40, no. 10, pp. 634-642, 1993. <https://doi.org/10.1109/82.246164>
- [7] H. Yang, W. K. Tang, G. Chen, and G.-P. Jiang, "Multi-carrier chaos shift keying: System design and performance analysis", *IEEE Transactions on Circuits and Systems I: Regular Papers*, vol. 64, no. 8, pp. 2182-2194, 2017. <https://doi.org/10.1109/tcsi.2017.2685344>
- [8] G. Kaddoum, J. Olivain, G. B. Samson, P. Giard, and F. Gagnon, "Implementation of a differential chaos shift keying communication system in GNU radio", in *2012 International Symposium on Wireless Communication Systems (ISWCS)*, 2012: IEEE, pp. 934-938. <https://doi.org/10.1109/iswcs.2012.6328505>
- [9] G. Kaddoum, F.-D. Richardson, and F. Gagnon, "Design and analysis of a multi-carrier differential chaos shift keying communication system", *IEEE Transactions on Communications*, vol. 61, no. 8, pp. 3281-3291, 2013. <https://doi.org/10.1109/tcomm.2013.071013.130225>
- [10] P. Chen, L. Wang, and F. C. Lau, "One analog STBC-DCSK transmission scheme not requiring channel state information", *IEEE Transactions on Circuits and Systems I: Regular Papers*, vol. 60, no. 4, pp. 1027-1037, 2013. <https://doi.org/10.1109/tcsi.2012.2209304>
- [11] Y. Xia, C. K. Tse, and F. C.-M. Lau, "Performance of differential chaos-shift-keying digital communication systems over a multipath fading channel with delay spread", *IEEE Transactions on Circuits and Systems II: Express Briefs*, vol. 51, no. 12, pp. 680-684, 2004. <https://doi.org/10.1109/tcsii.2004.838329>
- [12] S. Wang and X. Wang, "M-DCSK-based chaotic communications in MIMO multipath channels with no channel state information", *IEEE Transactions on Circuits and Systems II: Express Briefs*, vol. 57, no. 12, pp. 1001-1005, 2010. <https://doi.org/10.1109/tcsii.2010.2083091>
- [12] Z. Galias and G. M. Maggio, "Quadrature chaos-shift keying: Theory and performance analysis", *IEEE Transactions on Circuits and Systems I: Fundamental Theory and Applications*, vol. 48, no. 12, pp. 1510-1519, 2001. <https://doi.org/10.1109/tcsi.2001.972858>
- [13] H. Yang and G.-P. Jiang, "High-efficiency differential-chaos-shift-keying scheme for chaos-based noncoherent communication", *IEEE Transactions on Circuits and Systems II: Express Briefs*, vol. 59, no. 5, pp. 312-316, 2012. <https://doi.org/10.1109/tcsii.2012.2190859>
- [14] W. Xu, L. Wang, and G. Kolumbán, "A new data rate adaption communications scheme for code-shifted differential chaos shift keying modulation", *International Journal of Bifurcation and Chaos*, vol. 22, no. 08, p. 1250201, 2012. <https://doi.org/10.1142/s021812741250201x>
- [15] W. Xu, L. Wang, and C.-Y. Chi, "A simplified GCS-DCSK modulation and its performance optimization", *International Journal of Bifurcation and Chaos*, vol. 26, no. 13, p. 1650213, 2016. <https://doi.org/10.1142/s0218127416502138>
- [16] G. Kaddoum and F. Gagnon, "Design of a high-data-rate differential chaos-shift keying system", *IEEE Transactions on Circuits and Systems II: Express Briefs*, vol. 59, no. 7, pp. 448-452, 2012. <https://doi.org/10.1109/tcsii.2012.2198982>
- [17] L. Wang, G. Cai, and G. R. Chen, "Design and performance analysis of a new multiresolution M-ary differential chaos shift keying communication system", *IEEE Transactions on Wireless Communications*, vol. 14, no. 9, pp. 5197-5208, 2015. <https://doi.org/10.1109/twc.2015.2434820>
- [18] G. Cai, Y. Fang, and G. Han, "Design of an adaptive multiresolution M-ary DCSK system", *IEEE Communications Letters*, vol. 21, no. 1, pp. 60-63, 2016. <https://doi.org/10.1109/lcomm.2016.2614682>
- [19] G. Cai, Y. Fang, G. Han, F. C. Lau, and L. Wang, "A square-constellation-based M-ary DCSK communication system", *IEEE Access*, vol. 4, pp. 6295-6303, 2016. <https://doi.org/10.1109/access.2016.2612224>

- [20] G. Kaddoum, E. Soujeri, and Y. Nijssure, "Design of a short reference noncoherent chaos-based communication systems", *IEEE Transactions on Communications*, vol. 64, no. 2, pp. 680-689, 2016. <https://doi.org/10.1109/tcomm.2015.2514089>
- [21] T. J. Wren and T.-C. Yang, "Orthogonal chaotic vector shift keying in digital communications", *IET Communications*, vol. 4, no. 6, pp. 739-753, 2010. <https://doi.org/10.1049/iet-com.2009.0122>
- [22] F. S. Hasan, "Design and analysis of an orthogonal chaotic vectors based differential chaos shift keying communication system", *Al-Nahrain Journal for Engineering Sciences*, vol. 20, no. 4, pp. 952-958, 2017. <https://doi.org/10.1109/access.2018.2862862>
- [23] G. Kaddoum and E. Soujeri, "NR-DCSK: A noise reduction differential chaos shift keying system", *IEEE Transactions on Circuits and Systems II: Express Briefs*, vol. 63, no. 7, pp. 648-652, 2016. <https://doi.org/10.1109/tcsii.2016.2532041>
- [24] S. Li, Y. Zhao, and Z. Wu, "Design and Analysis of an OFDM-based Differential Chaos Shift Keying Communication System", *J. Commun.*, vol. 10, no. 3, pp. 199-205, 2015. <https://doi.org/10.12720/jcm.10.3.199-205>
- [25] F. S. Hasan, "Design and analysis of an OFDM-based short reference quadrature chaos shift keying communication system", *Wireless Personal Communications*, vol. 96, no. 2, pp. 2205-2222, 2017. <https://doi.org/10.1007/s11277-017-4293-1>
- [26] F. S. Hasan and A. A. Valenzuela, "Design and analysis of an OFDM-based orthogonal chaotic vector shift keying communication system", *IEEE Access*, vol. 6, pp. 46322-46333, 2018. <https://doi.org/10.1109/access.2018.2862862>
- [27] E. Basar, "Index modulation techniques for 5G wireless networks", *IEEE Communications Magazine*, vol. 54, no. 7, pp. 168-175, 2016. <https://doi.org/10.1109/mcom.2016.7509396>
- [28] E. Soujeri, G. Kaddoum, M. Au, and M. Herceg, "Frequency index modulation for low complexity low energy communication networks", *IEEE Access*, vol. 5, pp. 23276-23287, 2017. <https://doi.org/10.1109/access.2017.2713721>
- [29] W. Xu and L. Wang, "CIM-DCSK: A differential chaos shift keying scheme with code-index modulation", in *2016 16th International Symposium on Communications and Information Technologies (ISCIT)*, 2016: IEEE, pp. 100-104. <https://doi.org/10.1109/iscit.2016.7751600>
- [30] W. Xu, Y. Tan, F. C. Lau, and G. Kolumbán, "Design and optimization of differential chaos shift keying scheme with code index modulation", *IEEE Transactions on Communications*, vol. 66, no. 5, pp. 1970-1980, 2018. <https://doi.org/10.1109/tcomm.2018.2805342>
- [31] W. Xu, T. Huang, and L. Wang, "Code-shifted differential chaos shift keying with code index modulation for high data rate transmission", *IEEE Transactions on Communications*, vol. 65, no. 10, pp. 4285-4294, 2017. <https://doi.org/10.1109/tcomm.2017.2725261>
- [32] Y. Tan, W. Xu, T. Huang, and L. Wang, "A multilevel code shifted differential chaos shift keying scheme with code index modulation", *IEEE Transactions on Circuits and Systems II: Express Briefs*, vol. 65, no. 11, pp. 1743-1747, 2017. <https://doi.org/10.1109/tcsii.2017.2764916>
- [33] G. Cheng, L. Wang, W. Xu, and G. Chen, "Carrier index differential chaos shift keying modulation", *IEEE Transactions on Circuits and Systems II: Express Briefs*, vol. 64, no. 8, pp. 907-911, 2016. <https://doi.org/10.1109/tcsii.2016.2613093>
- [34] G. Cheng, L. Wang, Q. Chen, and G. Chen, "Design and performance analysis of generalised carrier index M-ary differential chaos shift keying modulation", *IET Communications*, vol. 12, no. 11, pp. 1324-1331, 2018. <https://doi.org/10.1049/iet-com.2017.0800>
- [35] W. Dai, H. Yang, Y. Song, and G. Jiang, "Two-layer carrier index modulation scheme based on differential chaos shift keying", *IEEE Access*, vol. 6, pp. 56433-56444, 2018. <https://doi.org/10.1109/access.2018.2872748>
- [36] M. Au, G. Kaddoum, F. Gagnon, and E. Soujeri, "A joint code-frequency index modulation for low-complexity, high spectral and energy efficiency communications", *arXiv preprint arXiv:1712.07951*, 2017. <https://doi.org/10.1109/access.2017.2713721>
- [37] M. Herceg, D. Vranješ, G. Kaddoum, and E. Soujeri, "Commutation code index DCSK modulation technique for high-data-rate communication systems", *IEEE Transactions on Circuits and Systems II: Express Briefs*, vol. 65, no. 12, pp. 1954-1958, 2018. <https://doi.org/10.1109/tcsii.2018.2817930>
- [38] M. Herceg, G. Kaddoum, D. Vranješ, and E. Soujeri, "Permutation index DCSK modulation technique for secure multiuser high-data-rate communication systems", *IEEE Transactions on Vehicular Technology*, vol. 67, no. 4, pp. 2997-3011, 2017. <https://doi.org/10.1109/tvt.2017.2774108>
- [39] H. Ma, Y. Fang, P. Chen, S. Mumtaz, and Y. Li, "A novel differential chaos shift keying scheme with multidimensional index modulation", *IEEE Transactions on Wireless Communications*, vol. 22, no. 1, pp. 237-256, 2022. <https://doi.org/10.1109/tcomm.2022.3169214>
- [40] Y. Tao, Y. Fang, H. Ma, S. Mumtaz, and M. Guizani, "Multi-carrier DCSK with hybrid index modulation: A new perspective on frequency-index-aided chaotic communication", *IEEE Transactions on Communications*, vol. 70, no. 6, pp. 3760-3773, 2022. <https://doi.org/10.1109/tcomm.2022.3169214>
- [41] Y. Fang, J. Zhuo, H. Ma, S. Mumtaz, and Y. Li, "Design and analysis of a new index-modulation-aided DCSK system with frequency-and-time resources", *IEEE Transactions on Vehicular Technology*, 2023. <https://doi.org/10.1109/tvt.2023.3238379>
- [42] F. S. Hasan, "Design and analysis of grouping subcarrier index modulation for differential chaos shift keying communication system", *Physical Communication*, vol. 47, p. 101325, 2021. <https://doi.org/10.1016/j.phycom.2021.101325>
- [43] B. Nazar and F. S. Hasan, "Joint Grouping Subcarrier and Permutation Index Modulations Based Differential Chaos Shift Keying System", *Physical Communication*, vol. 61, p. 102213, 2023. <https://doi.org/10.1016/j.phycom.2023.102213>
- [44] X. Cai, W. Xu, L. Wang, and F. Xu, "Design and performance analysis of differential chaos shift keying system with dual-index modulation", *IEEE Access*, vol. 7, pp. 26867-26880, 2019. <https://doi.org/10.1109/access.2019.2901016>
- [45] M. Au, G. Kaddoum, M. S. Alam, E. Basar, and F. Gagnon, "Joint code-frequency index modulation for IoT and multi-user communications", *IEEE Journal of Selected Topics in Signal Processing*, vol. 13, no. 6, pp. 1223-1236, 2019. <https://doi.org/10.1109/jstsp.2019.2933056>
- [46] J. G. Proakis, M. Salehi, *Digital Communications*, McGraw-Hill, New York, NY, USA, 2007.



**Ruaa Abdulkareem Yaseen** was born in Diyala, Iraq in 1992. She received her B.Sc. degree in Electronic Engineering from Diyala University, Iraq in 2014. She is currently pursuing an M.Sc. degree in Electronic and Communication Engineering at Al-Mustansiriyah University. Her research interests include Wireless Communication Systems, Index Modulation, and Chaotic Modulation.



**Fadhil S. Hasan** was born in Baghdad, Iraq in 1978. He received a B.Sc. degree in Electrical Engineering in 2000 and his M.Sc. degree in Electronics and Communication Engineering in 2003, both from the Mustansiriyah University, Iraq. He received a Ph.D. degree in 2013 in Electronics and Communication Engineering from the Basrah University, Iraq. In 2005, he joined the faculty of Engineering at Al-Mustansiriyah University in Baghdad. His recent research activities are Wireless Communication Systems, Multicarrier Systems, Wavelet based OFDM, MIMO Systems, Speech and Image Signal Processing, Chaotic Cryptography, Chaotic Modulation, FPGA, and Xilinx System Generator based Communication Systems. Now he has been a Prof. at Al-Mustansiriyah University.